

Raman scattering study of $(\text{K}_x\text{Sr}_{1-x})\text{Fe}_2\text{As}_2$ ($x = 0.0, 0.4$)

A. P. Litvinchuk^{1,2}, V. G. Hadjiev^{1,3}, M. N. Iliev^{1,2}, Bing Lv^{1,4}, A. M. Guloy^{1,4}, and C. W. Chu^{1,2,5}

¹Texas Center for Superconductivity at the University of Houston, TX 77204-5002

²Department of Physics, University of Houston, Texas 77204

³Department of Mechanical Engineering, University of Houston, Texas 77204

⁴Department of Chemistry, University of Houston, Texas 77204

⁵Hong Kong University of Science and Technology, Hong Kong, China

(Dated: November 23, 2021)

Polarized Raman spectra of non-superconducting SrFe_2As_2 and superconducting $\text{K}_{0.4}\text{Sr}_{0.6}\text{Fe}_2\text{As}_2$ ($T_c = 37$ K) are reported. All four phonon modes ($A_{1g} + B_{1g} + 2E_g$) allowed by symmetry, are found and identified. Shell model gives reasonable description of the spectra. No detectable anomalies are observed near the tetragonal-to-orthorhombic transition in SrFe_2As_2 or the superconducting transition in $\text{K}_{0.4}\text{Sr}_{0.6}\text{Fe}_2\text{As}_2$.

PACS numbers: 74.72.-b, 74.25.Kc, 63.20.D-, 78.30.-j

The renewed interest in superconductors was sparked recently by the discovery of a novel class of iron-arsenide based oxypnictides $\text{RFeAsO}_{1-x}\text{F}_x$ (where R is a rare earth element).[1, 2, 3, 4, 5] Similarly to the cuprate superconductors, doping of superconducting FeAs planes in oxypnictides determines one of the key characteristics of a given material, its superconducting transition temperature, which reaches values as high as $T_c = 54$ K. Oxypnictides were shown to exhibit n -type conductivity. More recently a series of compounds with similarly structured FeAs planes, but different charge reservoir block, $\text{A}_x\text{M}_{1-x}\text{Fe}_2\text{As}_2$ (where A is an alkali element and M - Sr or Ba) were found to exhibit superconducting properties.[6] Unlike oxypnictides these new superconductors clearly show p -type conductivity.[7] Optimal material doping is achieved in this later system at $x \approx 0.4 - 0.5$ when the critical temperature reaches $T_c \sim 38$ K.[8]

First principle electronic band structure calculations of oxypnictides point toward unconventional superconductivity, that is mediated by antiferromagnetic spin fluctuations[9, 10, 11]. Due to rather weak electron-phonon interactions it is generally believed that the phonons do not contribute substantially to the superconductivity. Despite this fact, it is important to experimentally identify the symmetry and frequency of phonon excitations and search for specific features in the Raman scattering spectra, which could shed light onto the properties of the superconducting state. In this communication we report the results of polarized Raman scattering studies of $(\text{K}_x\text{Sr}_{1-x})\text{Fe}_2\text{As}_2$ for the parent $x = 0$ compound and superconducting material with $x = 0.4$. We also present the results of shell model lattice dynamics calculations, which are in a good agreement with the experimental data.

The compounds under investigation were prepared by high-temperature solid state reactions of high purity K and Sr with FeAs, as described elsewhere.[8] For the mixed-metal samples, $(\text{K}_x\text{Sr}_{1-x})\text{Fe}_2\text{As}_2$, stoichiometric amounts of the ternary iron arsenides were thoroughly mixed, pressed and then annealed within welded Nb con-

tainers (jacketed in quartz) at about 900 C for 70-120 hours. The polycrystalline samples containing microcrystals of typical size $50 \times 50 \times 2 \mu\text{m}^3$ were characterized by X-ray diffraction, resistivity, magnetic susceptibility, Hall and thermoelectric power measurements.[8, 12] Raman scattering measurements were performed with a triple Horiba JY T64000 spectrometer, equipped with an optical microscope and liquid-nitrogen-cooled CCD detector. Samples were mounted on the cold finger of an optical cryostat. He-Ne laser ($\lambda_{\text{las}} = 638.2\text{nm}$) was used for the excitation and the power density did not exceed 10^4 W/cm^2 in order to minimize heating of the sample. Similarly to the case of RFeAsO [13] the Raman intensities were very low and required long acquisition time.

AFe_2As_2 crystallizes in the tetragonal ThCr_2Si_2 type structure with space group $I4/mmm$ (D_{4h}^{17}).[14] The unit parameters and atomic positions were obtained from powder diffraction data, using Rietveld refinement. The atomic positions were consistent with the literature values. The cell parameters for SrFe_2As_2 are $a = 0.39259(2)$ nm, $c = 1.2375(1)$ nm, for $\text{K}_{0.40}\text{Sr}_{0.60}\text{Fe}_2\text{As}_2$ are $a = 0.38898(2)$ nm, $c = 1.2948(1)$ nm; $z_{\text{As}} = 0.3516$ for both compounds. The structure features individual FeAs layers identical to those in RFeAsO , but with a different layer stacking sequence (AA in RFeAsO , and AB in the ThCr_2Si_2 -type structure).

From symmetry considerations[15] one expects four Raman-active phonons: $A_{1g}(\text{As})$, $B_{1g}(\text{Fe})$, $E_g(\text{As})$, and $E_g(\text{Fe})$ (Table I). Using the polarization selection rules and the fact that the ab surfaces could easily be visually recognized, the identification of the Raman line symmetry is straightforward. In particular, in the spectra obtained from the ab plane the intensity of the A_{1g} mode will remain constant for any orientation of the incident polarization \vec{e}_i given that the scattered polarization \vec{e}_s is parallel to it ($\vec{e}_s \parallel \vec{e}_i$) and will be zero in any crossed polarization configuration ($\vec{e}_s \perp \vec{e}_i$). The intensity of the B_{1g} mode, however, depends on the angle α between \vec{e}_i and the a -axis being proportional to $\cos^2 2\alpha$ for parallel and $\sin^2 2\alpha$ for crossed configuration. Figure 1 shows the variations with α of the Raman spectra of SrFe_2As_2

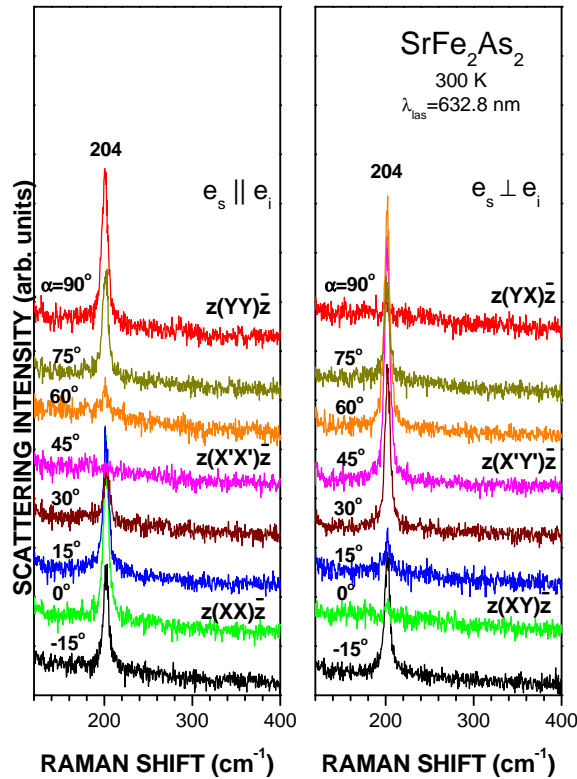


FIG. 1: (Color online) Raman spectra of SrFe_2As_2 for a series of ab -plane polarized scattering geometries. Numbers on the left denote the angle α between incident light polarization and the crystallographic a -axis.

obtained from the ab plane. Only one line at 204 cm^{-1} is clearly pronounced in the spectra and its intensity follows the angular dependence expected for the B_{1g} mode. Obviously, the intensity of the A_{1g} mode is negligible for incident light propagating along the c -axis and polarized in the ab plane. However, all Raman active phonons are clearly seen in the spectra taken from $ac(bc)$ surface, as illustrated in Fig. 2. These observations suggest the following relations between the elements of the Raman tensor in Table I: $|b| \gg |a|$ and $|c| \gg |a|$. The experimental phonon frequencies are listed in Table I.

We also performed shell model calculations of the lattice dynamics using the General Utility Lattice Program (GULP)[16], which is known to reasonably describe wide class of ionic materials, oxides in particular.[17, 18] In the shell model each ion is considered as a point core with charge Y surrounded by a massless shell with charge Q . The free ion polarizability is accounted for by the force constant k . The short range potentials $V(r)$ are chosen in the Born-Mayer-Buckingham form

$$V(r) = a \exp(-r/r_0) - cr^{-6}.$$

The model parameters of Fe^{2+} , Sr^{2+} and As^{3-} were tuned in order to achieve the best agreement with experimental even-parity phonon modes (to the best of

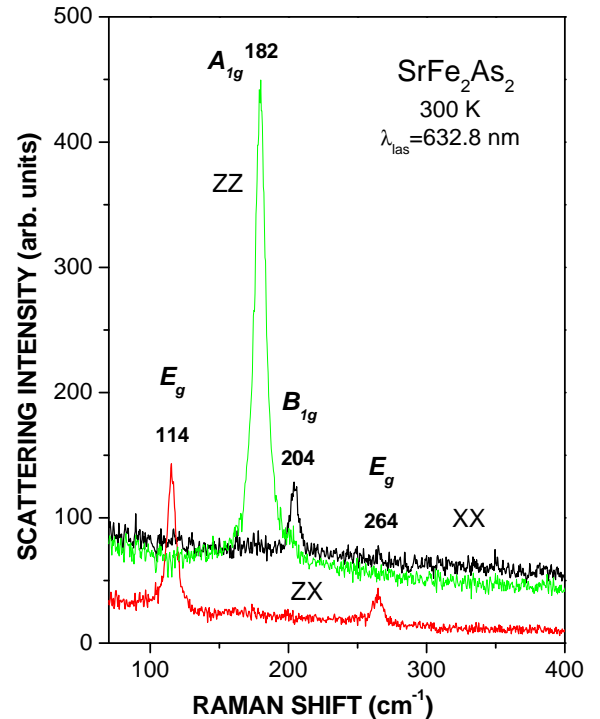


FIG. 2: XX (Color online) $A_{1g}+B_{1g}$ modes allowed), ZX (E_g), and ZZ (A_{1g}) spectra of SrFe_2As_2 , as obtained from ac surface at room temperature.

our knowledge, there is no experimental information on odd-parity infrared-active phonons); they are listed in Table II. The displacement patterns of all four Raman-active modes are shown in Fig. 3. It is worth noting here that while the A_{1g} and B_{1g} modes can be considered as "pure" modes, involving displacements along the c -axis of either As or only Fe, the two E_g modes are strongly mixed. As expected, the A_{1g} and B_{1g} modes of SrFe_2As_2 are very close in frequency to the corresponding modes of same symmetry in RFeAsO . [13] Indeed, the individual FeAs layers in both compounds are practically identical in term of bond lengths and angles.

Due to the small size of crystallites and long acquisition time, the Raman spectra of superconducting $\text{K}_{0.4}\text{Sr}_{0.6}\text{Fe}_2\text{As}_2$ ($T_c = 37\text{ K}$) could not be obtained in an exact scattering configuration and only the A_{1g} and B_{1g} modes were observed. Their frequency is practically the same as in the parent compound, the line width being somewhat larger. Upon lowering temperature these two modes show standard anharmonic behavior in both materials with rather moderate frequency and width variations as illustrated in Fig. 4 for $\text{K}_{0.4}\text{Sr}_{0.6}\text{Fe}_2\text{As}_2$. No phonon anomalies either near the tetragonal-to-orthorhombic structural transition of SrFe_2As_2 at $T_{t-o} \approx 203\text{ K}$ [19], or below $T_c=37\text{ K}$ of $\text{K}_{0.4}\text{Sr}_{0.6}\text{Fe}_2\text{As}_2$ were observed within the accuracy of our experiments for the A_{1g} and B_{1g} modes. In principle, the main effect of the structural transition should be a splitting of the E_g modes, which position was diffi-

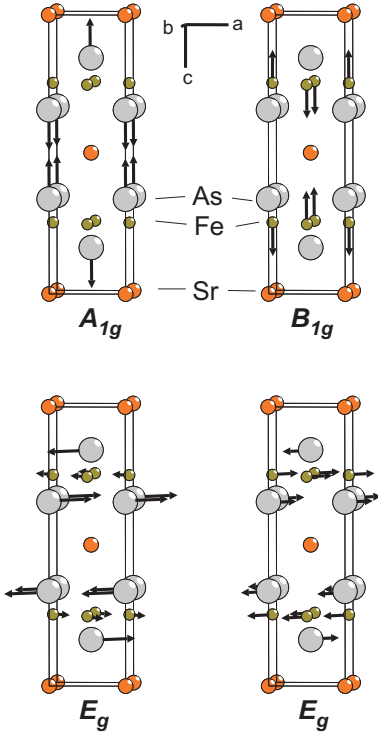


FIG. 3: (Color online) Displacement patterns of Raman-active modes of SrFe_2As_2 from the shell model calculations.

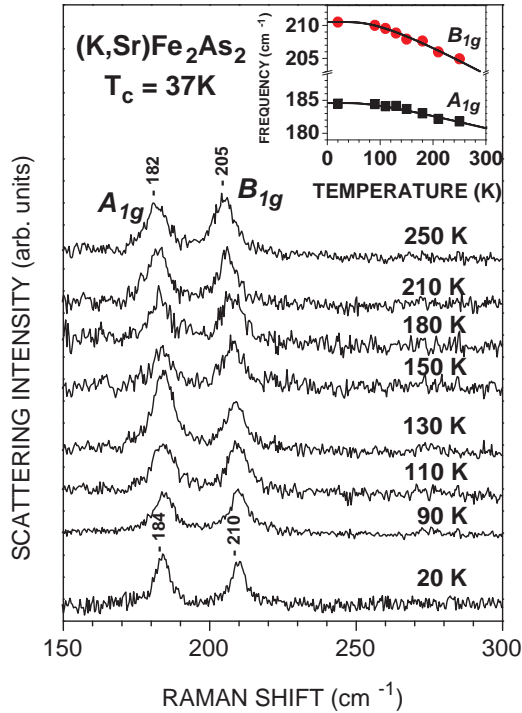


FIG. 4: (Color online) Temperature dependent Raman spectra of $\text{K}_{0.4}\text{Sr}_{0.6}\text{Fe}_2\text{As}_2$.

TABLE I: Wyckoff positions and irreducible representations for SrFe_2As_2 (space group $I4/mmm$, No.139), which yield Brillouin zone center modes. Lower part of the Table lists experimental and calculated mode frequencies and their activity.

Atom	Wyckoff position	Γ -point phonon modes
Sr	2a	$A_{2u} + E_u$
Fe	4d	$A_{2u} + B_{1g} + E_g + E_u$
As	4e	$A_{1g} + A_{2u} + E_g + E_u$

Modes classification:

$$\Gamma_{\text{Raman}} = A_{1g} + B_{1g} + 2E_g$$

$$\Gamma_{\text{IR}} = 2A_{2u} + 2E_u$$

$$\Gamma_{\text{Acoustic}} = A_{2u} + E_u$$

Raman tensors:

$$A_{1g}(x^2 + y^2, z^2) \rightarrow \begin{bmatrix} a & 0 & 0 \\ 0 & a & 0 \\ 0 & 0 & b \end{bmatrix}$$

$$B_{1g}(x^2 - y^2) \rightarrow \begin{bmatrix} c & 0 & 0 \\ 0 & -c & 0 \\ 0 & 0 & 0 \end{bmatrix}$$

$$E_{g1}(xz), E_{g2}(yz) \rightarrow \begin{bmatrix} 0 & 0 & -e \\ 0 & 0 & 0 \\ -e & 0 & 0 \end{bmatrix}, \begin{bmatrix} 0 & 0 & 0 \\ 0 & 0 & e \\ 0 & e & 0 \end{bmatrix}$$

Mode	Type	exp cm^{-1}	LDC cm^{-1}	Main atomic displacements	Allowed polarizations
A_{1g}	Raman	182	183	As(z)	XX, YY, ZZ
B_{1g}	Raman	204	203	Fe(z)	XX, YY, X'Y'
E_g	Raman	114	111	As(xy), Fe(xy)	XZ, YZ
E_g	Raman	264	335	Fe(xy), As(xy)	XZ, YZ
A_{2u}	IR		198	Sr(z), As(-z)	Z
A_{2u}	IR		322	Fe(z), Sr(-z)	Z
E_u	IR		135	Sr(xy)	X, Y
E_u	IR		263	Fe(xy), As(-xy)	X, Y

TABLE II: Shell model parameters and the short range potentials for SrFe_2As_2 . We used structural parameters reported in Ref. 8 and listed in the text.

Ion	$Y(e)$	$Q(e)$	$k(\text{eV} \times \text{\AA}^{-2})$	Ion pair	$a(\text{eV})$	$r_0(\text{\AA})$	$c(\text{eV} \times \text{\AA}^6)$
Sr	2.40	-0.50	10.0	Sr-As	1226	0.482	0
Fe	2.40	-0.50	19.9	Fe-As	2399	0.350	0
As	0.15	-3.00	15.2	As-As	2000	0.209	2500

cult to follow in the temperature-dependent experiments. The reported anisotropy of Fe-As bond lengths within ab-plane, however, is only 0.55% [19]. Following a simple expression [13] for the phonon frequency ω_{ph} as a function of bond length l : $\omega_{ph}^2 \sim 1/l^3$, one might expect splitting of the modes by about 0.8%. Even for the high frequency E_g mode at 264 cm^{-1} this yields 2.1 cm^{-1} , which is small compared to the linewidth and is challenging to be observed experimentally.

In conclusion, all four Raman active phonons in SrFe₂As₂ have been observed experimentally. The substitution of K for Sr has little effect on the frequencies of Raman modes involving As and Fe vibrations. The structural transition in SrFe₂As₂ and superconducting transition in K_{0.4}Sr_{0.6}Fe₂As₂ do not produce detectable anomalies in the parameters of A_{1g} and B_{1g} modes.

Acknowledgments

This work is supported in part by the T.L.L. Temple Foundation, the J.J. and R. Moores Endowment,

the State of Texas through TCSUH, the USAF Office of Scientific Research, and the LBNL through USDOE. B.L. and A.M.G. acknowledge the support from the NSF (CHE-0616805) and the R.A. Welch Foundation. We are grateful to Zhongjia Tang for help with crystallographic calculations.

-
- [1] Y. Kamihara, T. Watanabe, M. Hirano, and H. Hosono, *J. Am. Chem. Soc.* **130**, 3296 (2008).
 - [2] H. Takahashi, K. Igawa, K. Arii, Y. Kamihara, M. Hirano, and H. Hosono, *Nature* **453**, 376 (2008).
 - [3] X.H. Chen, T. Wu, G. Wu, R.H. Liu, H. Chen, and D.F. Fang, *Nature* **453**, 761 (2008).
 - [4] P.M. Grant, *Nature* **453**, 1000 (2008).
 - [5] T.Y. Chen, et al., *Nature* **453**, 1224 (2008).
 - [6] M. Rotter, M. Tegel and D. Johrendt, arXiv:0805.4630 (preprint).
 - [7] G.F. Chen, Z. Li, G. Li, W.Z. Hu, J. Dong, X.D. Zhang, P. Zheng, N.L. Wang, and J.L. Luo, arXiv:0806.1209 (preprint).
 - [8] K. Sasmal, B. Lv, B. Lorenz, A. Guloy, F. Chen, Y. Xue, C.W. Chu, arXiv:0806.1301 (preprint).
 - [9] D.J. Singh and M.H. Du, arXiv:0803.0429 (preprint).
 - [10] L. Boeri, O.V. Dolgov, and A.A. Golubov, arXiv:0803.2703 (preprint).
 - [11] I.I. Mazin, D.J. Singh, M.D. Johannes, and M.H. Du, arXiv:0803.2740v3 (preprint).
 - [12] B. Lorenz, B. Lv, and A.M. Guloy, unpublished results.
 - [13] V.G. Hadjiev, M.N. Iliev, K. Sasmal, Y.-Y. Sun, C.W. Chu, *Phys. Rev. B* **77**, 220505(R) (2008).
 - [14] S. Rozsa and H.U. Schuster, *Z. Naturforsch. B: Chem. Sci.* **36**, 1668 (1981).
 - [15] D.L. Rousseau, R.P. Bauman, and S.P.S. Porto, *J. Raman Spectr.* **10**, 253 (1981).
 - [16] G.D. Gale, *J. Chem. Soc. Faraday Trans.* **93**, 629 (1997).
 - [17] V.N. Popov, *J. Phys.: Cond. Matter* **7**, 1625 (1995).
 - [18] M.N. Iliev, M.V. Abrashev, A.P. Litvinchuk, V.G. Hadjiev, H. Guo, and A. Gupta, *Phys. Rev. B* **75**, 104118 (2007).
 - [19] M. Tegal, M. Rotter, V. Weiss, F.M. Schappacher, R. Pöttgen, and D. Johrendt, arXiv:0806.4782 (preprint).